THOR5th PMHS Abdomen Rigid Bar Tests

Test IDs: ABDRB01; ABDRB02; ABDRB03
Test Dates: August 28, 2018; October 16, 2018; December 05, 2018

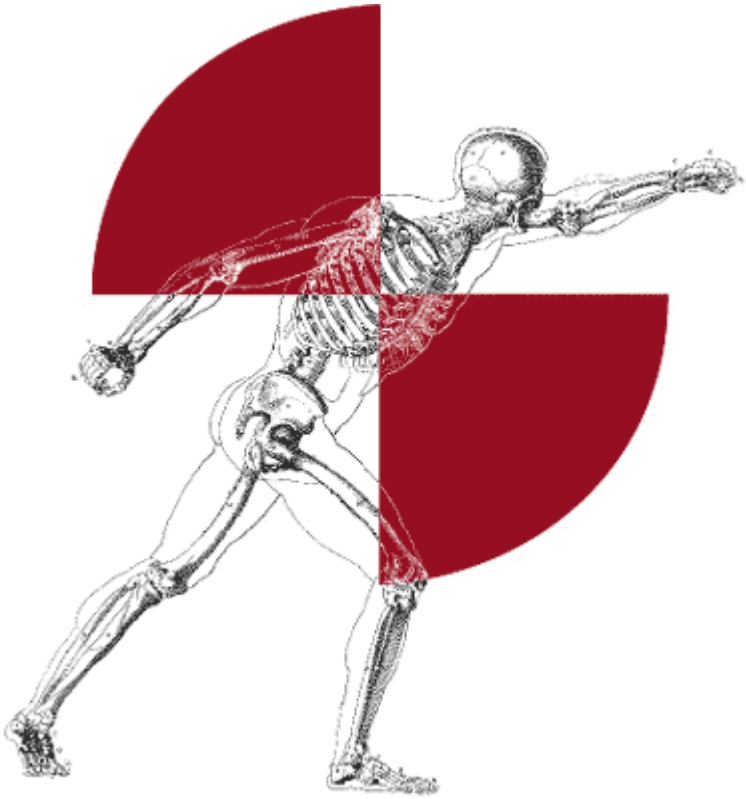

Prepared by:
Rakshit Ramachandra, PhD; John H Bolte IV, PhD
The Ohio State University
September 2019

Prepared for:
NHTSA

Section 1.0- Summary

Specific Aim:
This study evaluated the response of small post-mortem human surrogates (PMHS) subjected to an impactor loading test condition. The specimens were subjected to rigid bar impactor loading using a pneumatic ram, with the PMHS seated upright in a free-back configuration.

Overview:
This test report details the testing done on PMHS. This testing focused on characterizing the response of the abdomen when subjected to a rigid bar impact to the abdomen at a nominal velocity of 6 m/s. The fixture was replicated to mimic Hardy et al. (2001) setup, with the PMHS seated upright on a table with no back constraint. The test series was designed to load the abdomen in a non-injurious manner by limiting the compression to approximately 27% of the seated abdominal depth measured at the time of testing. The methodology used to test the PMHS in such a scenario is detailed throughout the report.

Section 2.0- Methods

Test Fixture:

The impactor loading device was designed to mimic Hardy et al (2001) setup for midabdominal impacts. A 2.5 cm diameter rigid bar impactor was attached to the ram shaft by means of a six degree of freedom load cell to measure the impact force. The force data was inertially compensated to account for the impactor face mass. Event tape was placed on both the subject and impactor face. When contact of the subject and impactor event tapes occurred, the data acquisition system was triggered and time zero defined. Just prior to impacting the PMHS, a magnetic bracket released the subject's head restraint allowing the subject to move freely after the impact. The rigid bar made initial contact with the PMHS at the umbilical region, approximately at the level of the umbilicus or L3.

PMHS Selection and Preparation:

A total of three PMHS were obtained through The Ohio State University's Body Donor Program and their use was approved by the Body Donor Program's Advisory Committee. All specimens were screened for infectious diseases, and a dual energy X-ray absorptiometry (DXA) scan was used to exclude specimens with osteoporosis. Specimens were required to have a body mass index (BMI) less than 29.9 and obese specimens were excluded. Specimens that had major abdominal scars or a history of abdominal disease were also excluded. A computed tomography (CT) scan was done prior to acceptance of each PMHS to check for pre-existing issues such as fractures or artificial implants. Testing on the PMHS11 and PMHS12 was performed within 72 to 120 hours post death, while PMHS13 was frozen fresh.

The specimens were stored in a cooler set at four degree Celsius overnight but were brought up to room temperature of twenty one degrees Celsius prior to firing. Anthropometry of the PMHS were measured and recorded. Abdominal measurements such as depth, circumference and width were taken during specimen evaluation. The abdominal depth measurements were taken again after positioning the subject in order to adjust the ram stroke. Prior to installing instrumentation, warm saline of around forty degrees

Celsius was flushed through both arterial and venous systems to clear all clots from the abdominal aorta and IVC. The saline used for vascular perfusion was measured to be thirty degree Celsius at the time of testing. The bladder and colon were not evacuated.

Instrumentation:

Internal instrumentation included pressure transducers (Millar instruments, TX, Model #SP-524) attached to angiographic catheters routed through Foley catheters. The pressure transducer assemblies were inserted into the abdominal aorta and inferior vena cava (IVC). To re-pressurize the abdominal region of each PMHS, Foley balloons in the venous system were inflated between the heart and liver in the IVC and just above the bifurcation of the iliac veins. In the aorta, Foley balloons were inflated around the level of 11th and 12th thoracic vertebrae and just above the bifurcation to iliac arteries. The CT scan images featuring the Foley balloon placement are shown in Appendix B.

The pressure transducers were then inserted into the vasculature to record pressure during the event. The pressure transducer locations included the superior IVC, inferior IVC (intersection of left and right common iliac veins), superior abdominal aorta (celiac trunk) and inferior abdominal aorta (intersection of left and right common iliac arteries).

In order to track the spinal motion, six degree-of-freedom (6 DOF) motion blocks to vertebrae T8, T12, L3 and L5 using bridge mounts that rested on the pedicles of the respective vertebrae with one screw drilled though the vertebral body. Figure 1 shows a representation of 6DOF motion blocks placed in the PMHS.

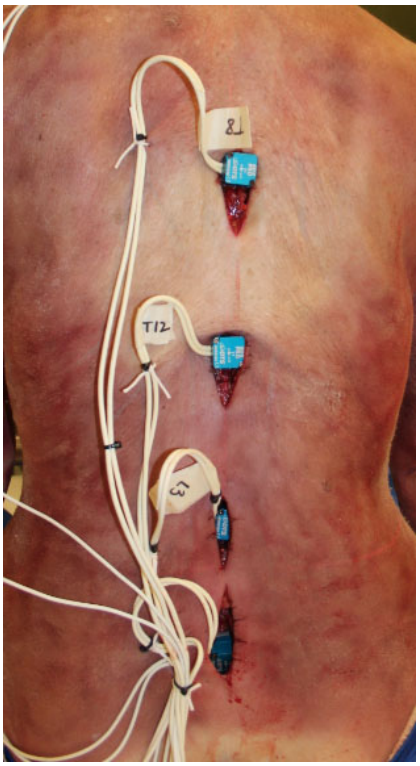

Figure 1: 6DOF motion blocks mounted on neural arch of 8th and 12th thoracic, and 3rd and 5th lumbar vertebrae

A linear displacement potentiometer mounted between the moving ram and its stationary frame measured ram displacement. The six-axis load cell and a linear accelerometer (Endevco, CA, Model #7264c) attached to the non-contacting surface of the impactor were used to obtain inertially compensated loading data. Data was either collected using a TDAS G5 or TDAS SlicePro data acquisition system (DTS, Seal Beach, CA).

Test Set-up:

Following instrumentation, a pre-test CT scan was done. The CT scan was used to document the locations of the internal instrumentation in addition to identify any pre-existing injuries or post-test damage to the skeleton where possible. Figure 2: shows the pre-test position of the PMHS. Once the instrumentation was complete and subject positioned on the test apparatus, a FARO Arm (FARO Technologies Inc., Florida) was used to document subject position in all three dimensions and locate the initial position of the key landmarks.

Prior to impact, the arms were lifted to shoulder level to ensure that they would not interfere with the impact or movement of the PMHS. The lumbar spine was positioned to be upright without any slouch and the legs splayed slightly outward in a natural seated position. The PMHS were kept in the seated position on a Teflon skid using a head halter connected to an electromagnet which was attached to the frame of the fixture.

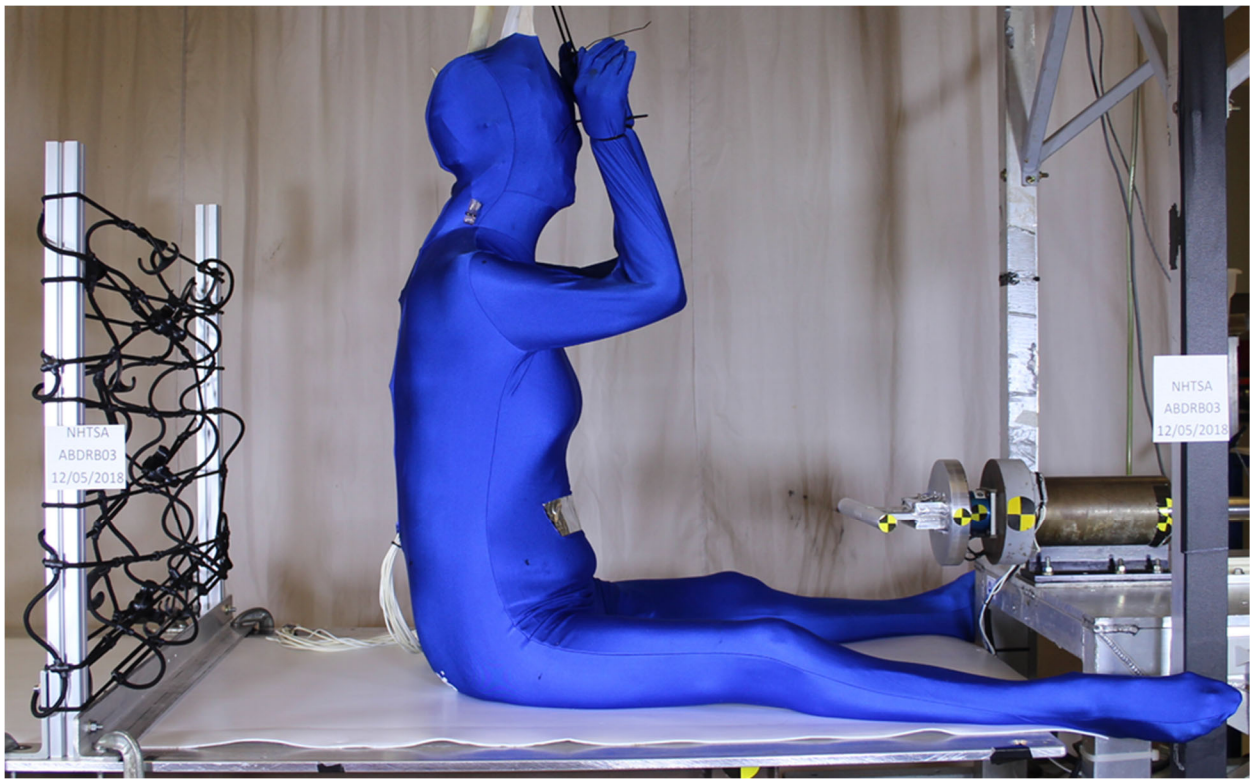

Figure 2: Pre-test positioning of PMHS13 on the impact test device

Both arterial and venous systems in the abdomen were re-pressurized using saline before each test to approximate physiological levels (14.0kPa in the aorta and 0.9kPa in the IVC). Upon release of the electromagnet, the pneumatic ram system was triggered and thus, the specimen was able to move freely

during the event.
The abdominal region of each specimen was loaded by the seatbelt at approximately 6 m/s. The penetration was intended to be limited to approximately 27% of seated abdominal depth measured after final positioning. This number was carried over from the previous non-injurious fixed-back belt pull test series where no injuries to abdominal organs were found. Each test was captured using high-speed camera (Vision Research Inc., NJ, Phantom at 1000fps) placed laterally to the specimen.

Damage Response:

Following the test performed on each PMHS, a post-test CT scan was taken to document the change in locations of the internal instrumentation as well as any damage that occurred. An anatomical dissection was then conducted to note all damage in detail. Injury severity scores were assigned based on Abbreviated Injury Scale 2005 – update 2008 (Gennarelli et al. 2008).

Data Analysis:

Data were acquired at a sampling frequency of 20,000 Hz and in the laboratory coordinate system (LCS), with the positive x-axis directed from posterior to anterior, positive y-axis directed from left to right, and positive z-axis directed from superior to inferior, per standard SAE-J211. Contact switch was attached to metal tapes on the impactor surface and the PMHS abdomen to trigger the event and this corresponded to time zero for all data including sensors and high-speed cameras.

Abdomen penetration was defined as the deflection of the abdomen versus time, where the deflection was measured at the point anterior to the abdomen at the sagittal midline using the ram potentiometer after impact. Abdomen penetration was calculated by subtracting the displacement of the third lumbar vertebrae by the displacement of the ram. Compression of the abdomen was defined as the percentage of penetration, calculated by dividing the abdominal penetration by initial abdominal depth measured just prior to firing each test. It must be noted that the seated abdomen depth varied between initial acceptance and just prior to firing the ram for the same specimen due to the perfusion of organs and vasculature.

Pressure readings in the abdominal aorta and IVC were recorded during each PMHS test. A fast Fourier Transform (FFT) analysis of the pressure signals was performed followed by filtering at CFC60. The peak rates of pressure change, $\dot{P}_{max}$, were calculated for IVC and compared with Ramachandra et al. (2016), where a value of 9.3 kPa/ms would correspond to a 50% risk of AIS 3+ abdominal injury.

Section 3.0- Results

A total of three tests were conducted on three postmortem human surrogates (PMHS). Table 1 shows pre-test characteristics of the tested PMHS. All of the PMHS were tested with vascular perfusion. PMHS11 and PMHS12 were used within 72 to 120 hours post death for testing while PMHS13 was used frozen fresh.

Table 1: Specimen information table (measurements listed are with the specimen in supine position at the time of acceptance)

Subject #	Test ID	Test Date	Age Sex	Mass (kg)	Stature (cm)	Abd C'ference (cm)	Abd Depth (cm)	Abd Width (cm)	BMI	L2-L4 BMD (T-Score)
PMHS11	ABDRB01	08/28/18	80F	61	165.1	81	20.2	31.4	22.3	+1.7
PMHS12	ABDRB02	10/16/18	77F	45	160	73.5	15.1	26.0	17.6	-1.5
PMHS13	ABDRB03	12/05/18	57F	51	159	78.5	17.4	27.2	20.2	-0.8
			Average	*52.3*	*161.4*	*77.7*	*17.6*	*28.2*	*20.0*	

Damage Response:

The anatomical dissection performed following each test revealed no damages to any of the abdominal organs after careful examination. ABDRB01 resulted in fractures to rib 5 on left side. It must be noted that this instance of skeletal damage is not considered for pressure based injury prediction since the risk function is based upon soft tissue damage in the abdomen and not related to skeletal damage.

Table 2: Damage summary (Abbreviated Injury Scale 2005 - Update 2008)

Test #	Abdominal	AIS	Skeletal	AIS
ABDRB01	None	0	Left 5th	1
ABDRB02	None	0	None	0
ABDRB03	None	0	None	0

Force-Penetration:

The force-time and penetration-time histories for the PMHS tests are shown in Figure 3 and Figure 4 respectively. Peak impact forces ranged from 1.07 to 1.46 kN. The peak penetrations ranged from 74 to 122 mm. Peak compression of the abdomen ranged from 39 to 49%. Figure 5 shows the non-normalized impact force vs. abdomen penetration responses. In all tests, it was noticed that the ram displaced beyond the hard stop set at 27% of the abdomen depth. This was especially pronounced in the test ABDRB01. The reason for the excess penetration may be attributed to the damping mechanism used to stop the impactor. A 55mm thick medium density polyurethane foam was used in ABDRB01 which was replaced with a 70 durometer Sorbothane rubber for tests ABDRB02 and 03. Although the overshoot occurs beyond the target point of interest, the data may be considered realistic at least until where the peak force is measured.

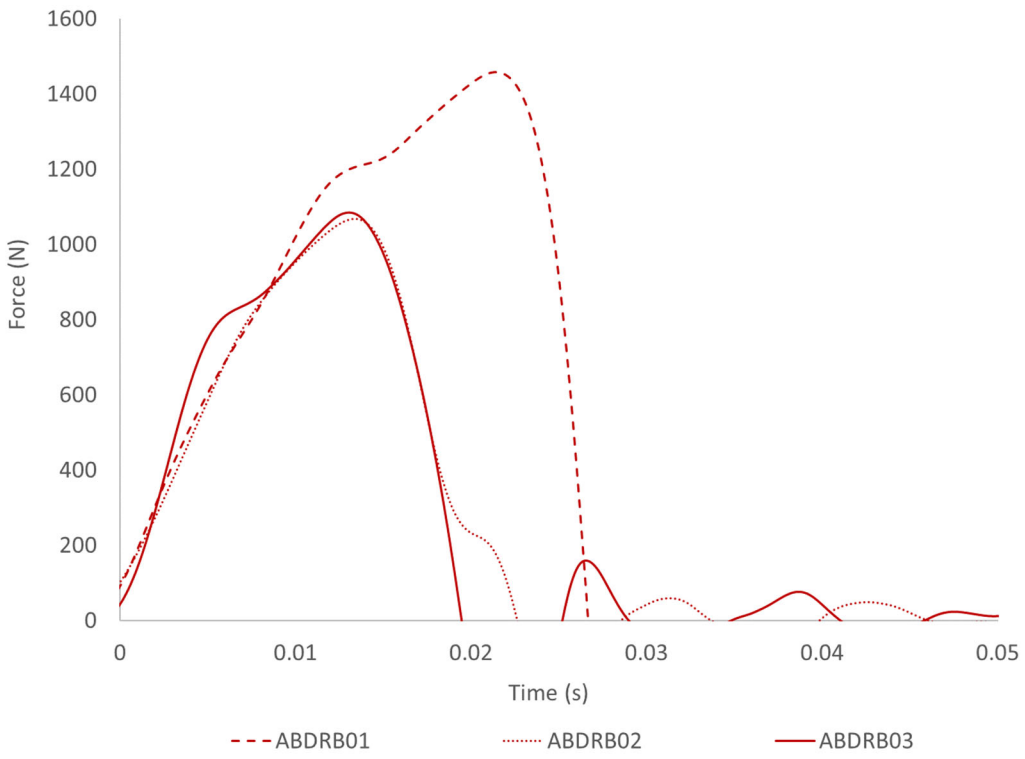

Figure 3: Force-time histories; ram force was calculated as: $F_{Ram\ comp} = F_{Ram} - F_{Ram\ beyond\ loadcell}$

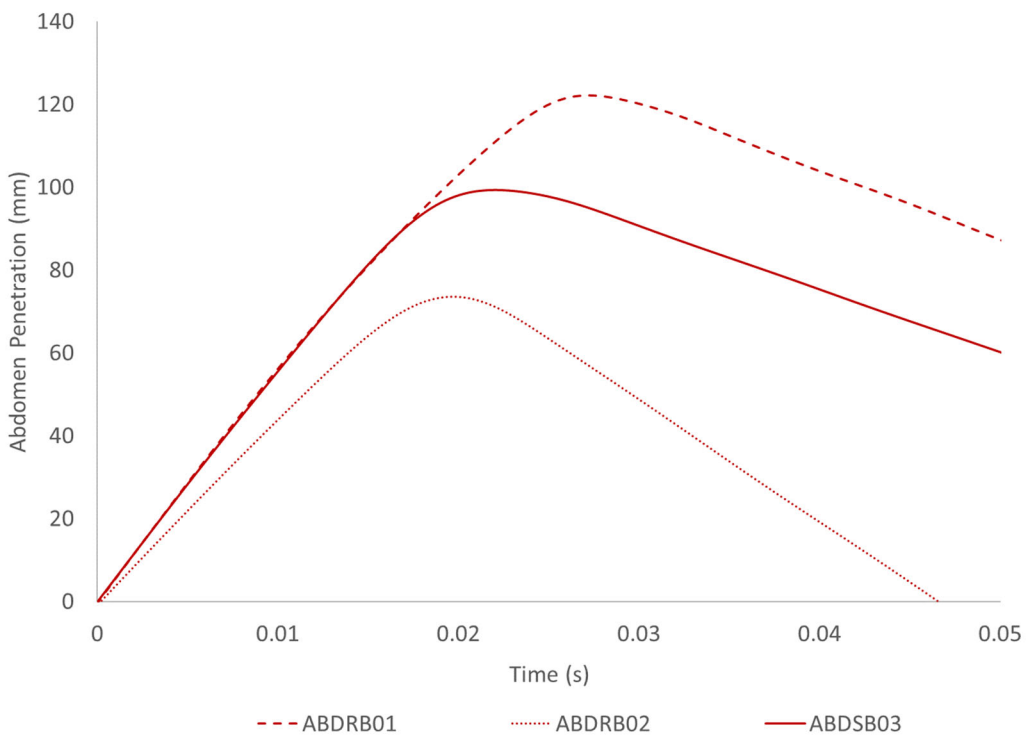

Figure 4: Abdomen penetration-time histories; abdomen penetration was calculated as: $\delta_{Abd} = \delta_{Ram} - \delta_{L3}$

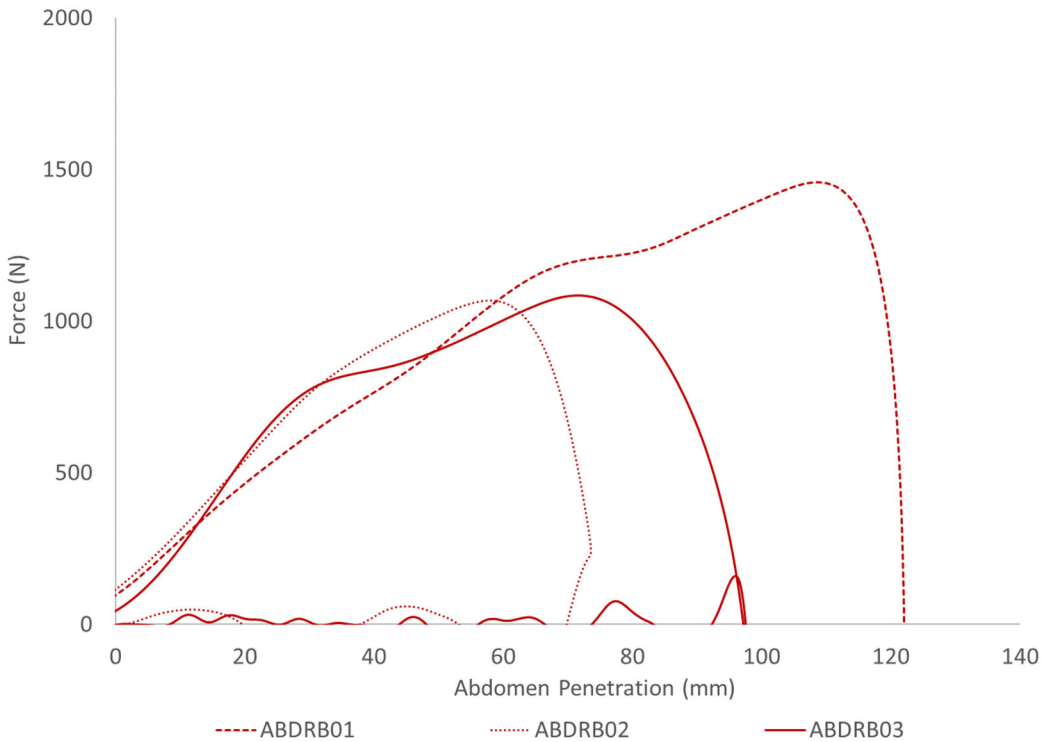

Figure 5: Impact force vs. abdomen penetration responses

Pressure:

For the perfusion pressure data, the pressure transducer with the highest peak (positive maximum) pressure was defined as P_{max}. The values of P_{max} from the abdominal aorta ranged from 11.5 to 50.0 kPa while the IVC transducers ranged from 16.0 to 44.0 kPa. The vascular pressure traces of all PMHS tests are presented in Appendix B. Data from the pressure transducers were used to calculate the positive maximum rate of pressure change ($\dot{P}_{max}$) during the event up to P_{max}. The $\dot{P}_{max}$ calculated for the IVC ranged from 2.52 to 5.47 kPa/ms. The calculated IVC $\dot{P}_{max}$ from all tests were less than 9.3 kPa/s which was a 50% abdominal injury risk value suggest by Ramachandra et al (2016).

Table 3 summarizes some of the commonly accepted biomechanical variables for injury risk prediction calculated from all PMHS tests and the corresponding peak values.

Table 3: Summary of peak responses and calculated biomechanical predictors

PMHS #	Belt Force (kN)	Penetration (mm)	Impact Speed (m/s)	Compression (%)	V_{max}*C_{max} (m/s)	F_{max}*C_{max} (kN)	IVC $\dot{P}_{max}$ (kPa/ms)	Abdomen MAIS
11	1.45	122	6.12	49	2.99	0.71	2.52	0
12	1.07	73	5.94	38	2.25	0.41	2.88	0
13	1.08	99	5.88	40	2.35	0.43	5.47	0

Section 4.0- Discussion

The general intent of this study was to load the abdomen in a non-injurious manner and obtain data to create an injury risk function (IRF) for the THOR-05F ATD, given its design and measurement capabilities such as the abdominal pressure sensors. This study conducted abdominal impact tests using three whole PMHS specimens in conditions like those described in Hardy et al. (2001). The rigid bar loading was applied at the umbilicus (approximately L3 vertebral height) and the subject was not restrained posteriorly. The target peak penetration of 27% was selected since it was unlikely to produce abdominal injuries based on the outcomes from previous part of this study. The objective was achieved since none of the three specimens sustained any abdominal injuries. Since the abdominal depths varied between PMHS at the time of testing, the penetration values were normalized by abdominal depths at the time of testing (Table 3) and the force vs. compression responses are shown in Figure 6.

Table 3: Abdominal depth measurements taken for restricting ram stroke

Subject #	Test ID	Abd Depth (cm)
PMHS11	ABDRB01	24.3
PMHS12	ABDRB02	18.5
PMHS13	ABDRB03	23.3

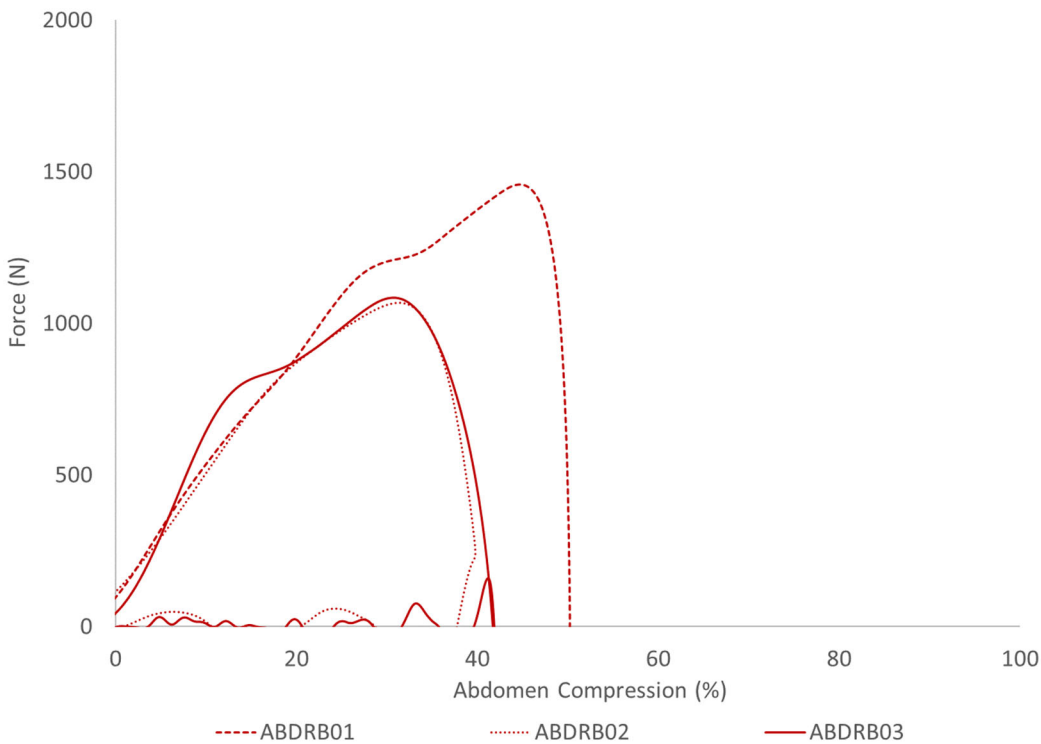

Figure 6: Impact force vs. abdomen compression responses

While the test apparatus was designed to mimic the Hardy et al. (2001) setup, due to the design limitations of the stopper mechanism, the actual penetration was greater than the desired 27%. Various damping techniques were investigated to reduce any damage to the fixture from a hard stop, including leather

padding, medium and high-density polyurethane foams and 70 durometer Sorbothane. The Sorbothane provided the shortest stroke beyond hard stop. However, since no injuries were observed from the three tests, the additional abdomen penetration was deemed acceptable. In terms of the biomechanical responses observed in the current study, it would translate directly to ATD tested when using the same test apparatus.

Section 5.0- Conclusion

A total of three rigid bar impact tests were conducted on three relatively small PMHS. The resulting nominal velocity at impact was 6 m/s.

- No abdominal organ damage occurred in any of the three tests, which was an intent of the study.
- The values of peak rate of vascular pressure change in conjunction with the lack of abdominal injuries obtained were consistent with the threshold of serious abdominal injuries as reported by Ramachandra et al. (2016).

Section 6.0- References

Hardy WN, Schneider LW, Rouhana SW (2001) Abdominal impact response to rigid bar, seatbelt, and airbag loading. Stapp Car Crash J 45:1–41.

Ramachandra et al., Biomechanical Responses of PMHS Subjected to Abdominal Seatbelt Loading, Stapp Car Crash J., 2016

APPENDIX A

Figure A1: 2.5cm diameter, 330mm long rigid bar impactor developed for this study

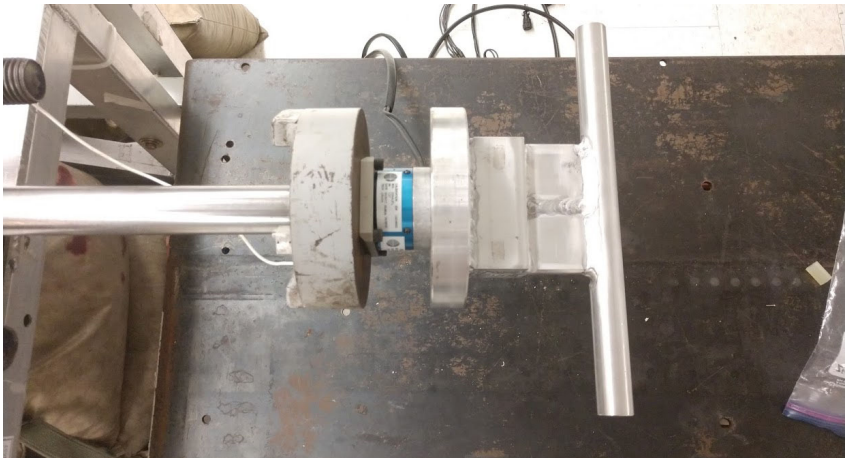

Figure A2: The rigid bar impactor attached to the pneumatic ram shaft by means of a six degree of freedom load cell

APPENDIX B

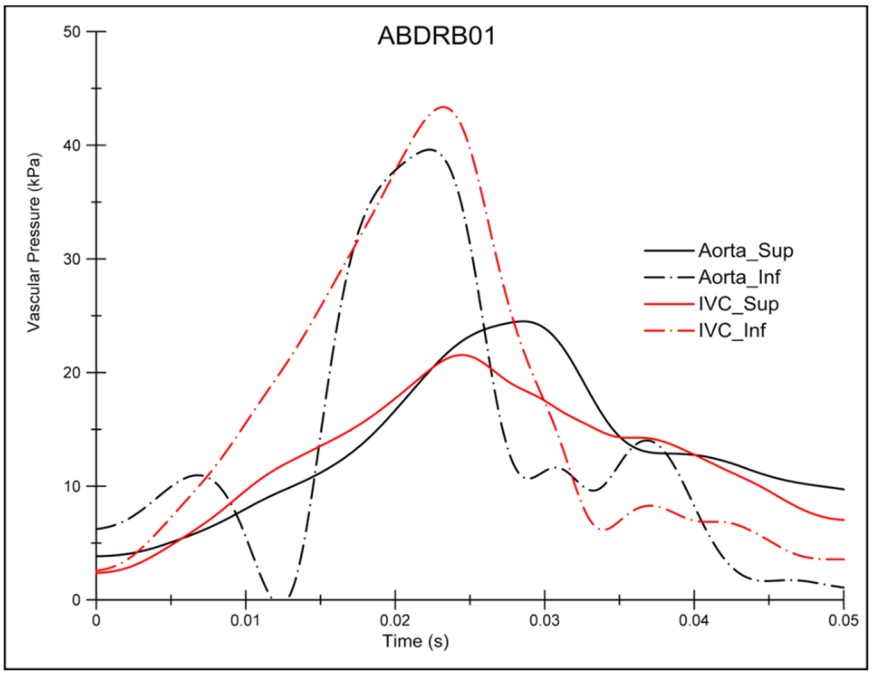

Figure B1: Vascular pressure traces (filtered at CFC60) from ABDRB01

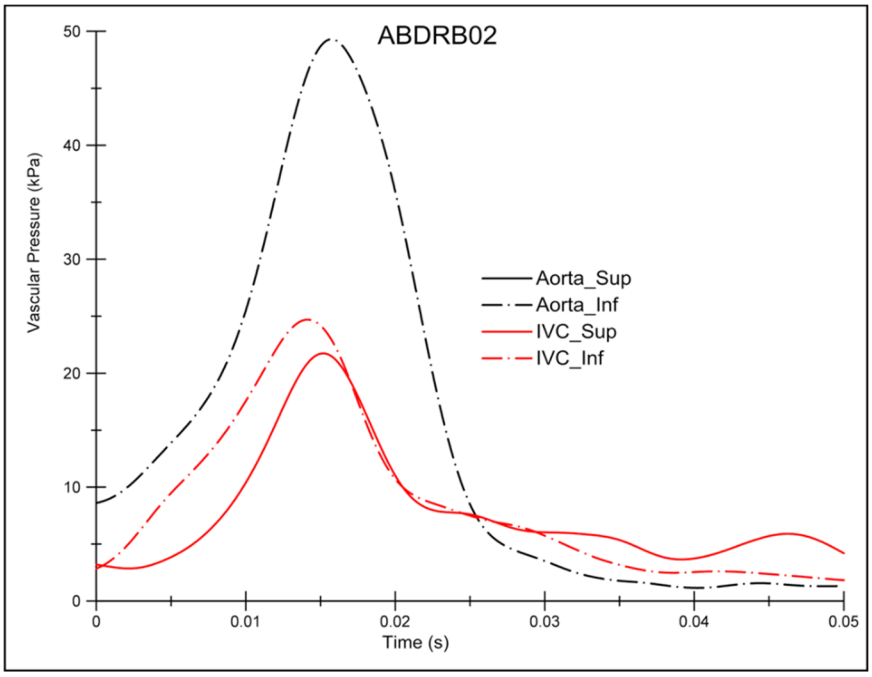

Figure B2: Vascular pressure traces (filtered at CFC60) from ABDRB02

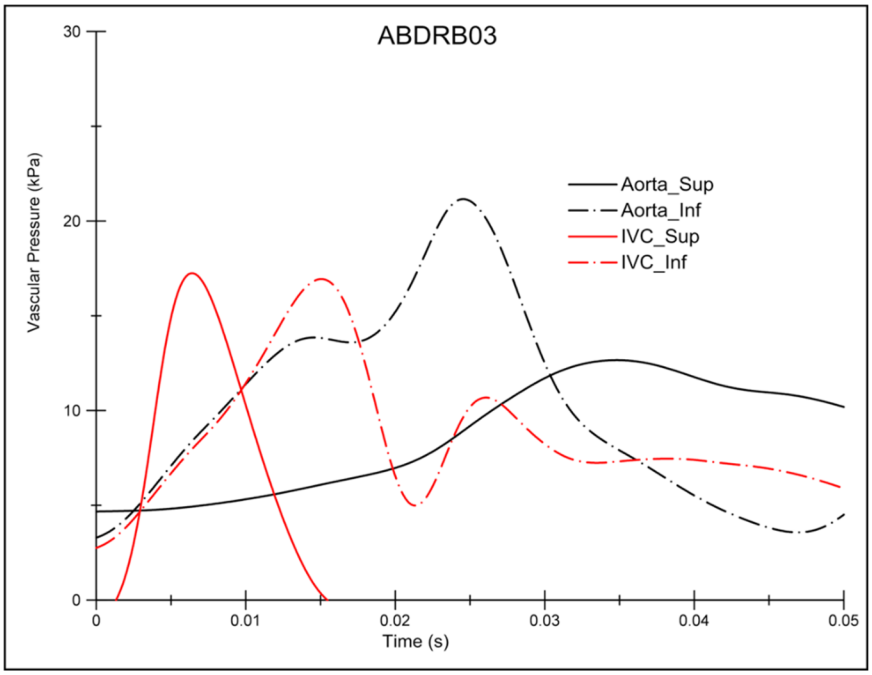

Figure B3: Vascular pressure traces (filtered at CFC60) from ABDRB03

Table B1: Peak pressure responses and calculated rate of pressure at each sensor location (filtered at CFC60)

Test#	Sensor Location	$\dot{P}_{max}$	P_{max} (kPa)
ABDRB01	aorta_sup	1.52	24.5
	aorta_inf	9.22	39.6
	IVC_sup	1.11	21.5
	IVC_inf	2.52	43.4
ABDRB02	aorta_sup	-	Sensor Fail
	aorta_inf	5.69	49.3
	IVC_sup	2.88	21.7
	IVC_inf	2.29	24.7
ABDRB03	aorta_sup	0.57	12.6
	aorta_inf	1.77	21.1
	IVC_sup	5.47	17.6
	IVC_inf	1.95	16.9

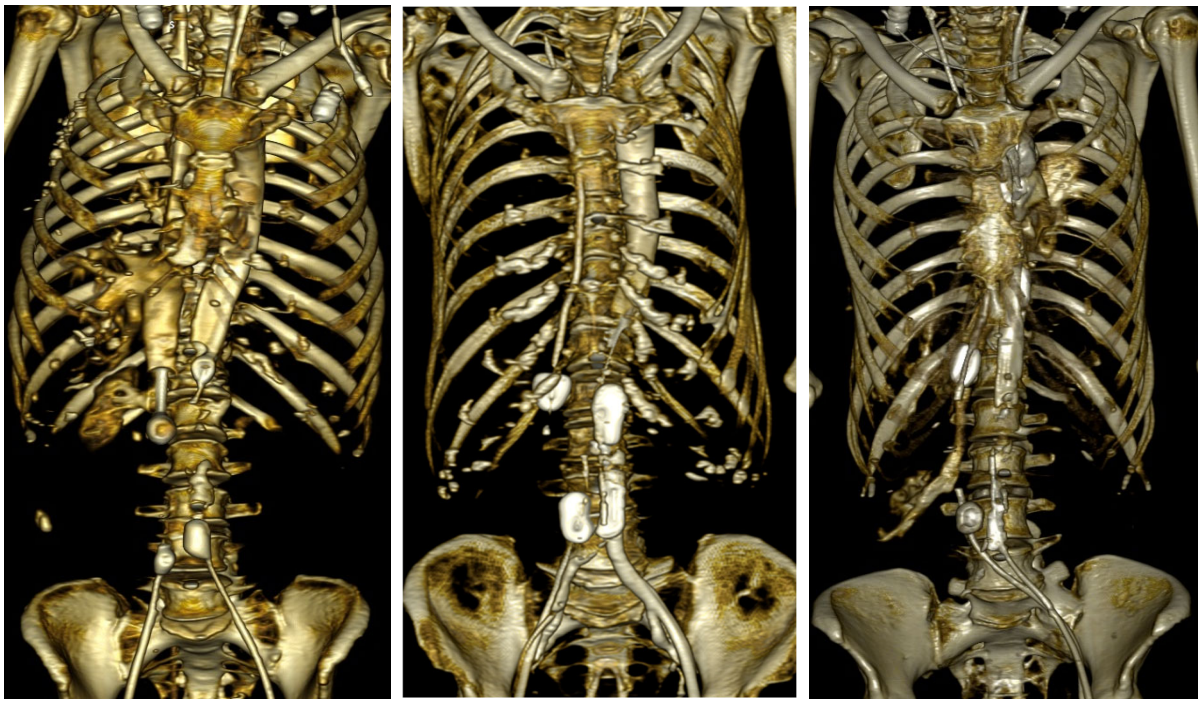

Figure B4: CT images with sensor and balloon locations in abdominal vasculature (left to right: PMHS11, 12, 13)

APPENDIX C

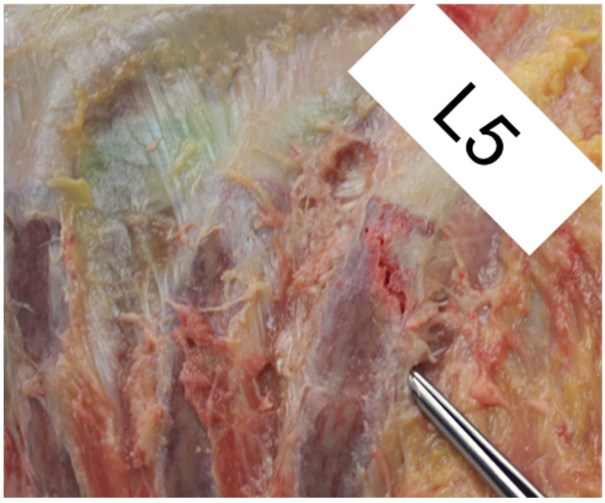

Figure C1: Skeletal damage on left 5th rib identified in ABDRB01 during anatomical dissection post testing

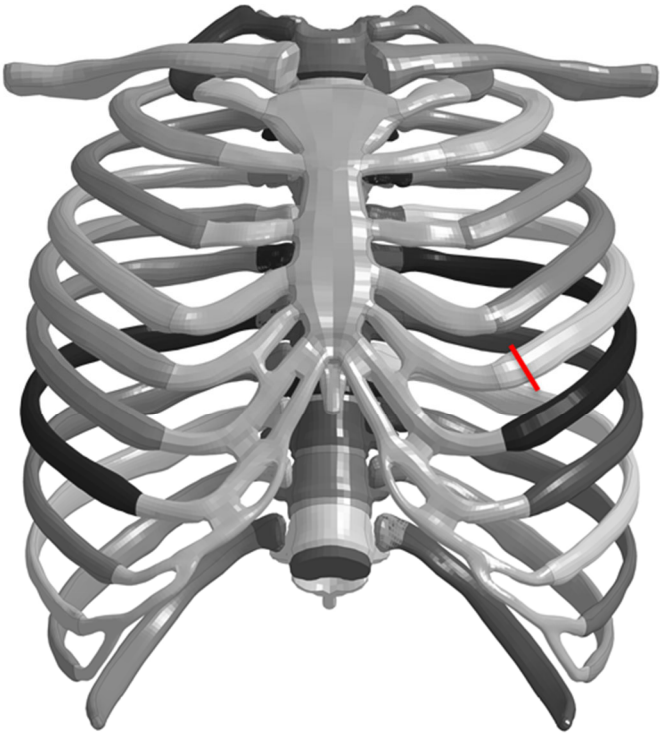

Figure C2: Skeletal damage locations identified in ABDRB01 during anatomical dissection post testing

APPENDIX D

ABDRB01

Channel#	Units	Sensor Manufacturer	Description
1	G'S	ENDEVCO	RAM XG
2	G'S	ENDEVCO	RAM XG - REDUNDANT
3	MM	PENNYGILES	RAM X DISPLACEMENT
4	NWT	HUMANETICS	RAM X FORCE
5	NWT	HUMANETICS	RAM Y FORCE
6	NWT	HUMANETICS	RAM Z FORCE
7	NWM	HUMANETICS	RAM X MOMENT
8	NWM	HUMANETICS	RAM Y MOMENT
9	NWM	HUMANETICS	RAM Z MOMENT
10	G'S	DTS	T8 X ACCELEROMETER (POSTERIOR) [6DX]
11	G'S	DTS	T8 Y ACCELEROMETER (POSTERIOR) [6DX]
12	G'S	DTS	T8 Z ACCELEROMETER (POSTERIOR) [6DX]
13	DPS	DTS	T8 X ANGULAR RATE SENSOR (POSTERIOR) [6DX]
14	DPS	DTS	T8 Y ANGULAR RATE SENSOR (POSTERIOR) [6DX]
15	DPS	DTS	T8 Z ANGULAR RATE SENSOR (POSTERIOR) [6DX]
16	G'S	DTS	T11 X ACCELEROMETER (POSTERIOR) [6DX]
17	G'S	DTS	T11 Y ACCELEROMETER (POSTERIOR) [6DX]
18	G'S	DTS	T11 Z ACCELEROMETER (POSTERIOR) [6DX]
19	DPS	DTS	T11 X ANGULAR RATE SENSOR (POSTERIOR) [6DX]
20	DPS	DTS	T11 Y ANGULAR RATE SENSOR (POSTERIOR) [6DX]
21	DPS	DTS	T11 Z ANGULAR RATE SENSOR (POSTERIOR) [6DX]
22	G'S	DTS	L3 X ACCELEROMETER (POSTERIOR) [6DX]
23	G'S	DTS	L3 Y ACCELEROMETER (POSTERIOR) [6DX]
24	G'S	DTS	L3 Z ACCELEROMETER (POSTERIOR) [6DX]
25	DPS	DTS	L3 X ANGULAR RATE SENSOR (POSTERIOR) [6DX]
26	DPS	DTS	L3 Y ANGULAR RATE SENSOR (POSTERIOR) [6DX]
27	DPS	DTS	L3 Z ANGULAR RATE SENSOR (POSTERIOR) [6DX]
28	G'S	DTS	L5 X ACCELEROMETER (POSTERIOR) [6DX]
29	G'S	DTS	L5 Y ACCELEROMETER (POSTERIOR) [6DX]
30	G'S	DTS	L5 Z ACCELEROMETER (POSTERIOR) [6DX]
31	DPS	DTS	L5 X ANGULAR RATE SENSOR (POSTERIOR) [6DX]
32	DPS	DTS	L5 Y ANGULAR RATE SENSOR (POSTERIOR) [6DX]
33	DPS	DTS	L5 Z ANGULAR RATE SENSOR (POSTERIOR) [6DX]
34	KPA	MILLAR	IVC (INFERIOR) PRESSURE
35	KPA	MILLAR	IVC (SUPERIOR) PRESSURE
36	KPA	MILLAR	AORTA (INFERIOR) PRESSURE
37	KPA	MILLAR	AORTA (SUPERIOR) PRESSURE

ABDRB02

Channel#	Units	Sensor Manufacturer	Description
1	NWT	HUMANETICS	RAM X FORCE
2	NWT	HUMANETICS	RAM Y FORCE
3	NWT	HUMANETICS	RAM Z FORCE
4	NWM	HUMANETICS	RAM X MOMENT
5	NWM	HUMANETICS	RAM Y MOMENT
6	NWM	HUMANETICS	RAM Z MOMENT
7	G'S	ENDEVCO	RAM XG
8	G'S	ENDEVCO	RAM XG REDUNDANT
9	MM	PENNYGILES	RAM X DISPLACEMENT
10	G'S	DTS	T8 X ACCELEROMETER (POSTERIOR) [6DX]
11	G'S	DTS	T8 Y ACCELEROMETER (POSTERIOR) [6DX]
12	G'S	DTS	T8 Z ACCELEROMETER (POSTERIOR) [6DX]
13	DPS	DTS	T8 X ANGULAR RATE SENSOR (POSTERIOR) [6DX]
14	DPS	DTS	T8 Y ANGULAR RATE SENSOR (POSTERIOR) [6DX]
15	DPS	DTS	T8 Z ANGULAR RATE SENSOR (POSTERIOR) [6DX]
16	G'S	DTS	T11 X ACCELEROMETER (POSTERIOR) [6DX]
17	G'S	DTS	T11 Y ACCELEROMETER (POSTERIOR) [6DX]
18	G'S	DTS	T11 Z ACCELEROMETER (POSTERIOR) [6DX]
19	DPS	DTS	T11 X ANGULAR RATE SENSOR (POSTERIOR) [6DX]
20	DPS	DTS	T11 Y ANGULAR RATE SENSOR (POSTERIOR) [6DX]
21	DPS	DTS	T11 Z ANGULAR RATE SENSOR (POSTERIOR) [6DX]
22	G'S	DTS	L3 X ACCELEROMETER (POSTERIOR) [6DX]
23	G'S	DTS	L3 Y ACCELEROMETER (POSTERIOR) [6DX]
24	G'S	DTS	L3 Z ACCELEROMETER (POSTERIOR) [6DX]
25	DPS	DTS	L3 X ANGULAR RATE SENSOR (POSTERIOR) [6DX]
26	DPS	DTS	L3 Y ANGULAR RATE SENSOR (POSTERIOR) [6DX]
27	DPS	DTS	L3 Z ANGULAR RATE SENSOR (POSTERIOR) [6DX]
28	G'S	DTS	L5 X ACCELEROMETER (POSTERIOR) [6DX]
29	G'S	DTS	L5 Y ACCELEROMETER (POSTERIOR) [6DX]
30	G'S	DTS	L5 Z ACCELEROMETER (POSTERIOR) [6DX]
31	DPS	DTS	L5 X ANGULAR RATE SENSOR (POSTERIOR) [6DX]
32	DPS	DTS	L5 Y ANGULAR RATE SENSOR (POSTERIOR) [6DX]
33	DPS	DTS	L5 Z ANGULAR RATE SENSOR (POSTERIOR) [6DX]
34	KPA	MILLAR	IVC (INFERIOR) PRESSURE
35	KPA	MILLAR	AORTA (INFERIOR) PRESSURE
36	KPA	MILLAR	IVC (SUPERIOR) PRESSURE
37	KPA	MILLAR	AORTA (SUPERIOR) PRESSURE

ABDRB03

Channel#	Units	Sensor Manufacturer	Description
1	MM	PENNYGILES	RAM X DISPLACEMENT
2	G'S	ENDEVCO	RAM XG
3	G'S	ENDEVCO	RAM XG REDUNDANT
4	NWT	HUMANETICS	RAM X FORCE
5	NWT	HUMANETICS	RAM Y FORCE
6	NWT	HUMANETICS	RAM Z FORCE
7	NWM	HUMANETICS	RAM X MOMENT
8	NWM	HUMANETICS	RAM Y MOMENT
9	NWM	HUMANETICS	RAM Z MOMENT
10	G'S	DTS	T8 X ACCELEROMETER (POSTERIOR) [6DX]
11	G'S	DTS	T8 Y ACCELEROMETER (POSTERIOR) [6DX]
12	G'S	DTS	T8 Z ACCELEROMETER (POSTERIOR) [6DX]
13	DPS	DTS	T8 X ANGULAR RATE SENSOR (POSTERIOR) [6DX]
14	DPS	DTS	T8 Y ANGULAR RATE SENSOR (POSTERIOR) [6DX]
15	DPS	DTS	T8 Z ANGULAR RATE SENSOR (POSTERIOR) [6DX]
16	G'S	DTS	T11 X ACCELEROMETER (POSTERIOR) [6DX]
17	G'S	DTS	T11 Y ACCELEROMETER (POSTERIOR) [6DX]
18	G'S	DTS	T11 Z ACCELEROMETER (POSTERIOR) [6DX]
19	DPS	DTS	T11 X ANGULAR RATE SENSOR (POSTERIOR) [6DX]
20	DPS	DTS	T11 Y ANGULAR RATE SENSOR (POSTERIOR) [6DX]
21	DPS	DTS	T11 Z ANGULAR RATE SENSOR (POSTERIOR) [6DX]
22	G'S	DTS	L3 X ACCELEROMETER (POSTERIOR) [6DX]
23	G'S	DTS	L3 Y ACCELEROMETER (POSTERIOR) [6DX]
24	G'S	DTS	L3 Z ACCELEROMETER (POSTERIOR) [6DX]
25	DPS	DTS	L3 X ANGULAR RATE SENSOR (POSTERIOR) [6DX]
26	DPS	DTS	L3 Y ANGULAR RATE SENSOR (POSTERIOR) [6DX]
27	DPS	DTS	L3 Z ANGULAR RATE SENSOR (POSTERIOR) [6DX]
28	G'S	DTS	L5 X ACCELEROMETER (POSTERIOR) [6DX]
29	G'S	DTS	L5 Y ACCELEROMETER (POSTERIOR) [6DX]
30	G'S	DTS	L5 Z ACCELEROMETER (POSTERIOR) [6DX]
31	DPS	DTS	L5 X ANGULAR RATE SENSOR (POSTERIOR) [6DX]
32	DPS	DTS	L5 Y ANGULAR RATE SENSOR (POSTERIOR) [6DX]
33	DPS	DTS	L5 Z ANGULAR RATE SENSOR (POSTERIOR) [6DX]
34	KPA	MILLAR	IVC (INFERIOR) PRESSURE
35	KPA	MILLAR	IVC (SUPERIOR) PRESSURE
36	KPA	MILLAR	AORTA (INFERIOR) PRESSURE
37	KPA	MILLAR	AORTA (SUPERIOR) PRESSURE